




# Oxidation of cysteine 117 stimulates constitutive activation of the type I $\alpha$ cGMP-dependent protein kinase

Received for publication, June 10, 2018, and in revised form, September 4, 2018. Published, Papers in Press, September 11, 2018, DOI 10.1074/jbc.RA118.004363

Jessica L. Sheehe<sup>‡</sup>, Adrian D. Bonev<sup>‡</sup>, Anna M. Schmoker<sup>§</sup>, Bryan A. Ballif<sup>§</sup>, Mark T. Nelson<sup>‡</sup>,  Thomas M. Moon<sup>¶1</sup>, and Wolfgang R. Dostmann<sup>‡2</sup>

From the <sup>‡</sup>Department of Pharmacology, Larner College of Medicine, and the <sup>§</sup>Department of Biology, University of Vermont, Burlington, Vermont 05405 and the <sup>¶</sup>Department of Chemistry and Biochemistry, University of Arizona, Tucson, Arizona 85721

Edited by Henrik G. Dohlman

The type I cGMP-dependent protein kinase (PKG I) is an essential regulator of vascular tone. It has been demonstrated that the type I $\alpha$  isoform can be constitutively activated by oxidizing conditions. However, the amino acid residues implicated in this phenomenon are not fully elucidated. To investigate the molecular basis for this mechanism, we studied the effects of oxidation using recombinant WT, truncated, and mutant constructs of PKG I. Using an *in vitro* assay, we observed that oxidation with hydrogen peroxide (H<sub>2</sub>O<sub>2</sub>) resulted in constitutive, cGMP-independent activation of PKG I $\alpha$ . PKG I $\alpha$  C42S and a truncation construct that does not contain Cys-42 ( $\Delta$ 53) were both constitutively activated by H<sub>2</sub>O<sub>2</sub>. In contrast, oxidation of PKG I $\alpha$  C117S maintained its cGMP-dependent activation characteristics, although oxidized PKG I $\alpha$  C195S did not. To corroborate these results, we also tested the effects of our constructs on the PKG I $\alpha$ -specific substrate, the large conductance potassium channel (K<sub>Ca</sub> 1.1). Application of WT PKG I $\alpha$  activated by either cGMP or H<sub>2</sub>O<sub>2</sub> increased the open probabilities of the channel. Neither cGMP nor H<sub>2</sub>O<sub>2</sub> activation of PKG I $\alpha$  C42S significantly increased channel open probabilities. Moreover, cGMP-stimulated PKG I $\alpha$  C117S increased K<sub>Ca</sub> 1.1 activity, but this effect was not observed under oxidizing conditions. Finally, we observed that PKG I $\alpha$  C42S caused channel flickers, indicating dramatically altered K<sub>Ca</sub> 1.1 channel characteristics compared with channels exposed to WT PKG I $\alpha$ . Cumulatively, these results indicate that constitutive activation of PKG I $\alpha$  proceeds through oxidation of Cys-117 and further suggest that the formation of a sulfur acid is necessary for this phenotype.

Blood pressure is maintained in part through constriction and relaxation of smooth muscle cells in the peripheral vasculature. During vasorelaxation, endothelium-derived nitric oxide or circulating natriuretic peptides activate guanylyl cyclase,

which produce cGMP (1). This second messenger binds to and activates the cGMP-dependent protein kinase I (PKG I),<sup>3</sup> a homodimeric enzyme that is expressed as two isoforms in vascular smooth muscle cells, PKG I $\alpha$  and I $\beta$  (2). PKG I $\alpha$  acts as a central regulator of vasorelaxation by modulating global and local Ca<sup>2+</sup> levels within the cell. Its phosphorylation targets include the large conductance calcium-activated potassium channel (BK<sub>Ca</sub>, K<sub>Ca</sub> 1.1), which causes membrane hyperpolarization and inhibition of voltage-dependent calcium channels (3–5). PKG I $\alpha$  also phosphorylates the myosin phosphatase-targeting subunit 1 (MYPT1), the small GTP-binding protein (RhoA), and the regulator of G-protein signaling 2 (RGS2), which mediate the downstream cytoskeletal rearrangement necessary for vascular relaxation (6–9).

This signaling cascade and physiological effects associated with cGMP-dependent activation of PKG I $\alpha$  are well-established (2). Under oxidizing conditions, PKG I $\alpha$  is known to be constitutively active (10–12). Several studies have suggested that a residue unique to the N terminus of PKG I $\alpha$ , Cys-42, may be the source of this activation (10, 13–15). The proposed mechanism involves the formation of an intermolecular disulfide bond between Cys-42 and Cys-42' from the opposing protomer in the homodimeric holoenzyme. Because this disulfide bond is located in the substrate targeting region of the kinase, it has been hypothesized that oxidation at this site also modulates targeting to substrates by altering the geometry of this domain (10, 11). These observations have been consequential toward understanding the role of oxidizing agents, such as hydrogen peroxide, in both physiological and pathophysiological processes within the vasculature (16–22).

Both activation and substrate targeting are required for PKG I-dependent signaling, and disruption of either is sufficient to alter normal physiological processes (23–26). In this study, we sought to isolate these two facets of PKG I $\alpha$  signaling by studying the effects of oxidation using recombinant WT, truncated, and mutant constructs of PKG I. We found that both PKG I $\alpha$  and I $\beta$  are activated by oxidation, although its effect on PKG I $\alpha$  is more pronounced. Furthermore, both PKG I $\alpha$  C42S and  $\Delta$ 53 PKG I $\alpha$  (a truncation mutant that does not contain Cys-42) are activated by oxidation. Using PKG I $\alpha$  C117S and C195S to test

This work was supported by National Institutes of Health Grants 5T32 HL007594-30 (to J. L. S.) and R01 HL121706 and R01 HL131181 (to M. T. N.) and additional support from the Totman Trust for Biomedical Research. The authors declare that they have no conflicts of interest with the contents of this article. The content is solely the responsibility of the authors and does not necessarily represent the official views of the National Institutes of Health.

This article contains Figs. S1–S5.

<sup>1</sup> To whom correspondence may be addressed. E-mail: [thomasmoon@email.arizona.edu](mailto:thomasmoon@email.arizona.edu).

<sup>2</sup> To whom correspondence may be addressed. E-mail: [wolfgang.dostmann@uvm.edu](mailto:wolfgang.dostmann@uvm.edu).

<sup>3</sup> The abbreviations used are: PKG I, cGMP-dependent protein kinase I; TCEP, tris(2-carboxyethyl)phosphine; PDB, Protein Data Bank; TEV, tobacco etch virus; MWCO, molecular weight cut-off; MeCN, acetonitrile; Xcorr, cross-correlation.

## Oxidation-dependent activation of PKG I $\alpha$ Cys-117

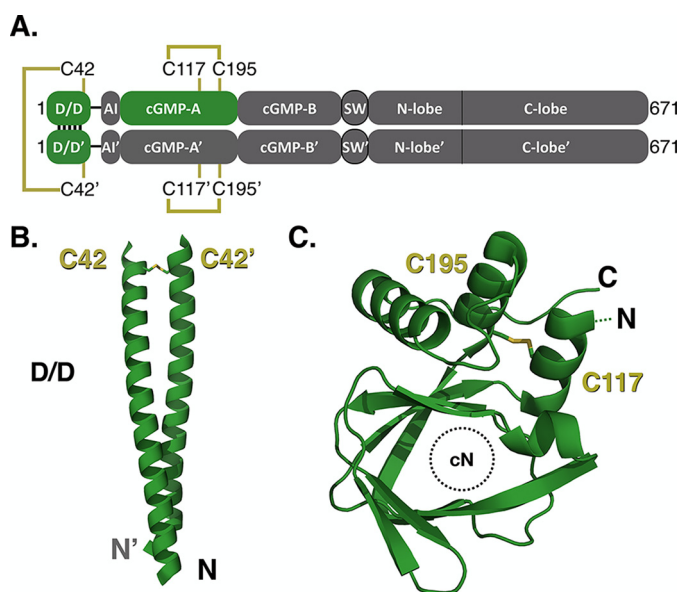


**Figure 1. Putative sites of oxidative activation in PKG I $\alpha$ .** A, linear domain diagram depicting the homodimeric PKG I $\alpha$  and the sites of cysteine residues hypothesized to be involved in the oxidative phenotype. B and C, structures denoting the location of disulfide bonds identified in the N-terminal dimerization domain (B) and the cGMP-A site (C) from PKG I $\alpha$  (PDB entries 4R4L and 3SHR, respectively).

the influence of a previously observed disulfide bond, we observed that oxidation at Cys-117 is necessary and sufficient for oxidative activation of PKG I $\alpha$ . Finally, we corroborated these *in vitro* results by measuring the PKG I $\alpha$ -dependent activation of the K<sub>Ca</sub> 1.1 channel. Taken together, these data support the hypothesis that constitutive activation of PKG I $\alpha$  via oxidation is not mediated through the interprotomer disulfide bond between Cys-42 and Cys-42', but rather through oxyacid formation at Cys-117 in the cGMP-A site.

## Results

### Oxidation of PKG I $\alpha$ abrogates cGMP-dependent activation

Under oxidizing conditions, there are two confirmed sites where disulfide bonds form in the PKG I $\alpha$  holoenzyme, which are an interprotomer disulfide bond between Cys-42 and Cys-42' and an intraprotomer disulfide bond between Cys-117 and Cys-195 (Fig. 1A) (11). These disulfide bonds have also been identified in recent structural studies of the isolated domains (Fig. 1, B and C) (11, 27, 28). The first disulfide bond between Cys-42 and Cys-42' forms at the C-terminal region of the dimerization domain (Fig. 1B). Cys-42 is one of four nonleucine/isoleucine residues at *d* positions within the coiled-coil and is unique to this isoform (Fig. S2A). The second disulfide bond in cGMP-A forms between Cys-117 and Cys-195 and is proximal to the cGMP-binding pocket (Fig. 1C and Fig. S2B).

To characterize the oxidative phenotype, recombinant PKG I $\alpha$  from *Sj9* cells was used for *in vitro* phosphotransferase assays, wherein changes in kinase activity could be monitored. First, we confirmed that PKG I $\alpha$  activity under reducing conditions (WT<sub>red</sub>) was consistent with previous studies (29, 30). Exposure to increasing concentrations of cGMP activated the kinase in a cooperative manner ( $n_H = 1.7$ ) by 20-fold with a half-maximal concentration of 200 nM (Fig. 2A and Table 1).

We next examined how increasing H<sub>2</sub>O<sub>2</sub> concentrations affected PKG I $\alpha$  activity. WT<sub>red</sub> was exposed to H<sub>2</sub>O<sub>2</sub>, and kinase activity was monitored under apo and saturating cGMP conditions (Fig. 2B). A maximum response was observed with 500  $\mu$ M H<sub>2</sub>O<sub>2</sub>, wherein we observed a reduction in the maximal velocity paired with a peak in the minimum velocity. At 1 mM H<sub>2</sub>O<sub>2</sub>, we observed a relative loss of activity in the presence and absence of cGMP, suggesting that exposure of the enzyme to this concentration of H<sub>2</sub>O<sub>2</sub> had compromised its catalytic function. To expand our understanding of the conditions in which to measure the oxidative phenotype, the -fold activation of PKG I $\alpha$  was monitored over a timed exposure to 500  $\mu$ M H<sub>2</sub>O<sub>2</sub> (Fig. 2C). After 30 min of exposure, we observed the greatest effect on the cGMP-dependent activation of the kinase, wherein the -fold activation was reduced by ~90% to 2.5 (Table 1). These conditions were used for all subsequent measurements of the oxidation phenotype.

Next, we tested the cGMP-dependent activation of oxidized PKG I $\alpha$ . Oxidation resulted in a 5–6-fold increase in basal activity in the absence of cGMP (1.13  $\mu$ mol/min  $\times$  mg;  $p < 0.001$  compared with WT<sub>red</sub>; Fig. 2A). In contrast, the addition of up to 4  $\mu$ M cGMP increased the activity by only 2.5-fold (2.77  $\mu$ mol/min  $\times$  mg). Moreover, the activation profile of WT<sub>ox</sub> with cGMP showed a decreased sensitivity for the cyclic nucleotide. In agreement with previous studies, analysis of WT PKG I $\alpha$  by nonreducing SDS-PAGE showed that increasing concentrations of H<sub>2</sub>O<sub>2</sub> resulted in formation of an interprotomer disulfide bond (Fig. 2D). In determining whether our PKG I constructs formed the interprotomer disulfide bond using nonreducing, SDS-PAGE electrophoresis, preliminary experiments indicated that removal of the reducing agent from the storage buffer would expose the enzymes to ambient air. Because prior studies have used ambient air to activate PKG I $\alpha$  by oxidation, we sought to avoid this contribution by retaining the reducing agent, tris(2-carboxyethyl)phosphine (TCEP), in the buffer and adding H<sub>2</sub>O<sub>2</sub> to levels that would overcome its reducing capacity (Fig. S1) (11, 35). Because TCEP is degraded by H<sub>2</sub>O<sub>2</sub> through oxidation to a phosphine oxide at a 1:1 ratio, the excess H<sub>2</sub>O<sub>2</sub> could be calculated (31, 32). Both the added (*black*) and final (H<sub>2</sub>O<sub>2</sub> minus TCEP; *red*) H<sub>2</sub>O<sub>2</sub> concentrations are shown.

### Cysteine mutants of PKG I $\alpha$ probe oxidation-induced constitutive activation

Next, we examined whether the oxidized phenotype in PKG I $\alpha$  is regulated by formation of the interprotomer disulfide bond between Cys-42 and Cys-42'. To achieve this, we measured the activities of reduced and oxidized PKG I $\alpha$  C42S (C42S<sub>red</sub> and C42S<sub>ox</sub>) (Fig. 3A and Table 1). When the mutant was measured under reducing conditions, we observed a basal activity similar to that of WT<sub>red</sub> (0.32  $\mu$ mol/min  $\times$  mg). However, when activated by cGMP, the maximal velocity was reduced by ~50% compared with WT<sub>red</sub> (2.31  $\mu$ mol/min  $\times$  mg), resulting in a 7-fold stimulation of activity. Moreover, C42S<sub>red</sub> showed a 3-fold shift in the activation constant ( $K_a = 580$  nM,  $p < 0.001$  compared with WT<sub>red</sub>) and a loss of cooperative, cGMP-dependent activation ( $n_H = 0.8$ ). For C42S<sub>ox</sub>, we observed a significant increase in basal activity (1.103  $\mu$ mol/

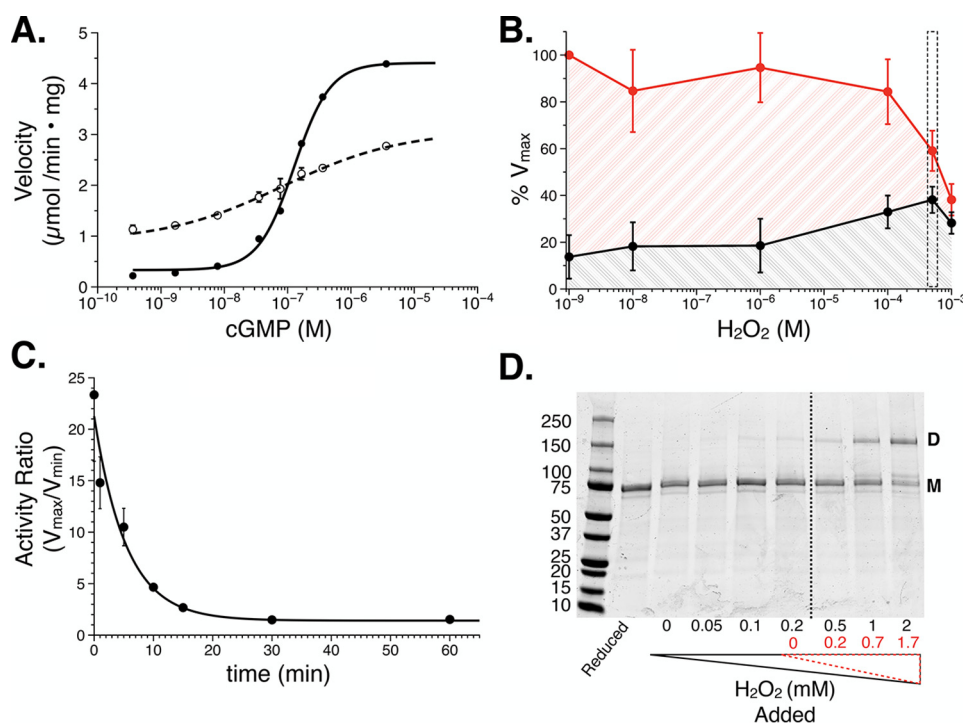


**Figure 2. Initial characterization of the PKG I $\alpha$  oxidative phenotype.** *A*, cGMP-dependent activation under reducing (solid line;  $n = 12$ ) and oxidizing (500  $\mu\text{M}$   $\text{H}_2\text{O}_2$ , 30 min; dashed line;  $n = 16$ ) conditions. *B*, PKG I $\alpha$  activity plotted against increasing concentrations of  $\text{H}_2\text{O}_2$ . Activity was measured in the absence (black;  $n = 4$ ) and presence of cGMP (red; 4  $\mu\text{M}$ ,  $n = 4$ ). The concentration of  $\text{H}_2\text{O}_2$  (500  $\mu\text{M}$ ) that resulted in the greatest increase in basal activity is highlighted in the boxed region. *C*, time course examining PKG I $\alpha$  oxidation with 500  $\mu\text{M}$  cGMP wherein the -fold activity ( $V_{\text{max}}/V_{\text{min}}$ ) was monitored ( $n = 4$ ). *D*, representative nonreducing, denaturing SDS-PAGE of PKG I $\alpha$  exposed to increasing concentrations of  $\text{H}_2\text{O}_2$ . The dashed line indicates the point at which the concentration of hydrogen peroxide overcomes the concentration of TCEP in the buffer.  $\text{H}_2\text{O}_2$  values corrected for the presence of TCEP are shown in red. Where shown, data are represented as the mean  $\pm$  S.D. (error bars).

**Table 1**  
cGMP-dependent phosphotransferase activity

Constructs	Reduced					Oxidized						
	$V_{\text{min}}^a$	$V_{\text{max}}^a$	$V_{\text{max}}/V_{\text{min}}$	$K_a^b$	$n_H^b$	$n$	$V_{\text{min}}^a$	$V_{\text{max}}^a$	$V_{\text{max}}/V_{\text{min}}$	$K_a^b$	$n_H^b$	$n$
	$\mu\text{mol}/\text{min} \times \text{mg}$	$\mu\text{mol}/\text{min} \times \text{mg}$		$\mu\text{M}$			$\mu\text{mol}/\text{min} \times \text{mg}$	$\mu\text{mol}/\text{min} \times \text{mg}$		$\mu\text{M}$		
<b>PKG I<math>\alpha</math></b>												
WT	0.22 $\pm$ 0.00	4.39 $\pm$ 0.03	20.0	0.20 $\pm$ 0.00	1.7 $\pm$ 0.0	12	1.13 $\pm$ 0.08	2.77 $\pm$ 0.03	2.5	NA	NA	16
C42S	0.32 $\pm$ 0.06	2.31 $\pm$ 0.18	7.3	0.58 $\pm$ 0.03	1.1 $\pm$ 0.1	14	1.10 $\pm$ 0.03	2.36 $\pm$ 0.11	2.1	0.13 $\pm$ 0.01	1.6 $\pm$ 0.2	6
$\Delta 53$	0.18 $\pm$ 0.16	3.95 $\pm$ 0.30	21.6	0.22 $\pm$ 0.03	0.9 $\pm$ 0.1	7	1.38 $\pm$ 0.19	1.58 $\pm$ 0.36	1.1	NA	NA	6
C117S	0.16 $\pm$ 0.10	4.09 $\pm$ 0.13	26.0	0.12 $\pm$ 0.01	1.4 $\pm$ 0.1	6	0.65 $\pm$ 0.14	3.81 $\pm$ 0.10	5.9	0.20 $\pm$ 0.00	1.2 $\pm$ 0.1	6
C195S	0.43 $\pm$ 0.02	4.67 $\pm$ 0.12	10.9	0.27 $\pm$ 0.01	1.8 $\pm$ 0.1	6	0.86 $\pm$ 0.02	3.20 $\pm$ 0.05	3.7	1.22 $\pm$ 0.11	0.8 $\pm$ 0.1	6
<b>PKG I<math>\beta</math></b>												
WT	0.04 $\pm$ 0.01	3.62 $\pm$ 0.26	86.1	1.21 $\pm$ 0.03	1.9 $\pm$ 0.1	7	0.42 $\pm$ 0.03	2.78 $\pm$ 0.10	6.6	0.86 $\pm$ 0.03	1.2 $\pm$ 0.1	6

<sup>a</sup> The velocity values indicate the  $\mu\text{mol}$  of peptide substrate (W15) phosphorylated/min/mg of PKG ( $\mu\text{mol}/\text{min} \times \text{mg}$ ) and are represented as the mean  $\pm$  S.D.

<sup>b</sup> Values were obtained from non-linear regression fit analyses and are represented as the means  $\pm$  standard deviations. Not applicable (NA) values indicate the data for that condition could not be fit to a non-linear regression.

min  $\times$  mg;  $p < 0.001$  compared with C42S<sub>red</sub>); however, the maximal activity was unchanged (2.357  $\mu\text{mol}/\text{min} \times \text{mg}$ ) and displayed kinetic characteristics similar to those of WT<sub>ox</sub>. Examination of C42S<sub>ox</sub> by nonreducing, denaturing SDS-PAGE did not show evidence of an intramolecular disulfide bond between protomers (Fig. 3E).

Due to the similar increases in basal activity between WT<sub>ox</sub> and C42S<sub>ox</sub> in response to  $\text{H}_2\text{O}_2$ , we next utilized  $\Delta 53$  PKG I $\alpha$ , a truncation construct of PKG I $\alpha$  that lacks the N terminus (and Cys-42) but retains cGMP-dependent activation (30).  $\Delta 53_{\text{red}}$  activity in the absence of cGMP was similar to WT PKG I $\alpha$  (Fig. 3B). In the presence of increasing concentrations of cGMP,  $\Delta 53$  activity increased by 20-fold with a  $K_a$  for cGMP that was similar to that of WT PKG I $\alpha$  (216 nM). When oxidized with  $\text{H}_2\text{O}_2$ ,  $\Delta 53_{\text{ox}}$  exhibited kinetic features similar to those of the WT<sub>ox</sub>

and C42S<sub>ox</sub> constructs. Specifically, the 7-fold increase in basal activity of  $\Delta 53_{\text{ox}}$  to 1.380  $\mu\text{mol}/\text{min} \times \text{mg}$  decreased its cGMP-dependent -fold activation to 1.1. Thus,  $\Delta 53$  displayed the highest sensitivity to oxidation. Like C42S, SDS-PAGE analyses showed that  $\Delta 53$  does not form an interprotomer disulfide bond in the presence of  $\text{H}_2\text{O}_2$  (Fig. 3E).

Because PKG I $\alpha$  and I $\beta$  are splice variants of the *prkg1* gene, within the same species, they are completely identical in their cGMP-binding and catalytic domains (with 98% sequence identity across placental mammals). However, their N-terminal dimerization, autoinhibitory, and linker regions only retain 26% sequence identity (Fig. S2). Thus, Cys-42 in the N terminus of I $\alpha$  is not conserved in PKG I $\beta$ . Upon ruling out the contribution of Cys-42 on the oxidation-dependent activation phenotype of PKG I $\alpha$ , we hypothesized that oxidative activation may origi-

## Oxidation-dependent activation of PKG I $\alpha$ -Cys-117

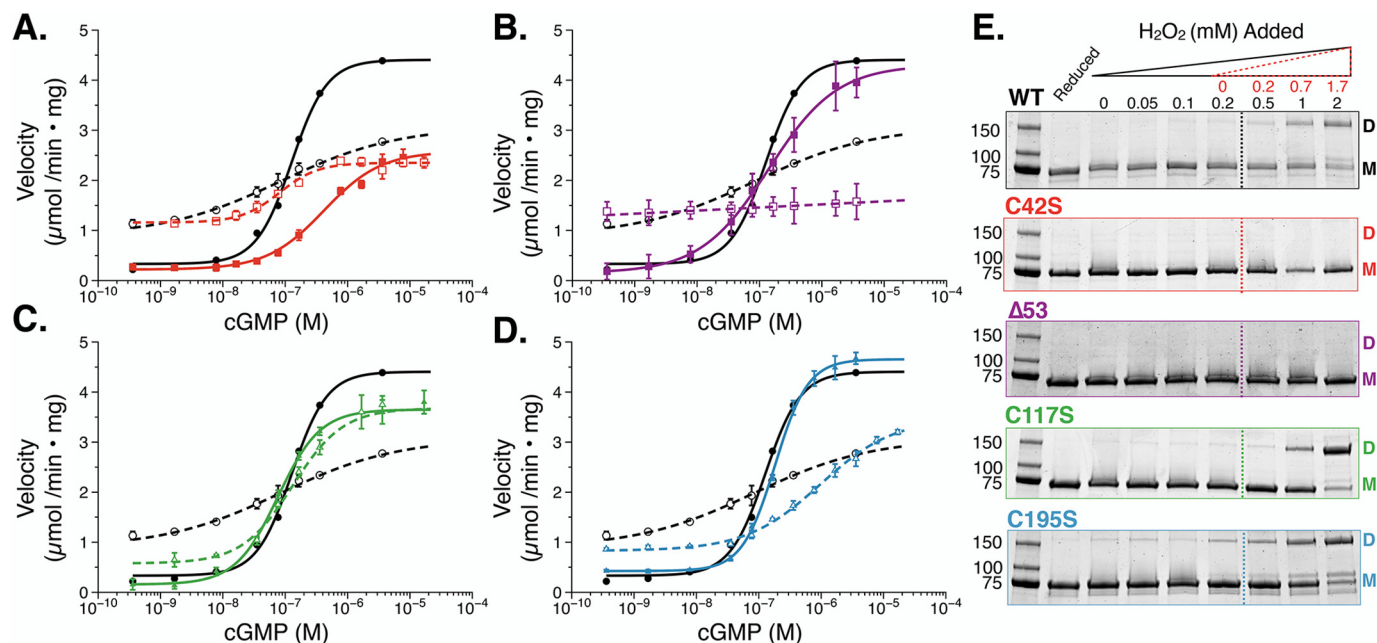


**Figure 3.** *In vitro* phosphotransferase assays of PKG I $\alpha$  under reducing and oxidizing conditions. A–D, cGMP-dependent activation of PKG I $\alpha$  WT (black circles) and PKG I $\alpha$  C42S (red squares) (A),  $\Delta 53$  PKG I $\alpha$  (purple squares) (B), PKG I $\alpha$  C117S (green triangles) (C), and PKG I $\alpha$  C195S (blue triangles) (D) under reducing (1 mM TCEP; solid lines) and oxidizing (500  $\mu\text{M}$   $\text{H}_2\text{O}_2$ , 30 min; dashed lines) conditions. Data are represented as the mean  $\pm$  S.D. (error bars). E, nonreducing, denaturing SDS-PAGE of PKG I $\alpha$  constructs treated with increasing concentrations of  $\text{H}_2\text{O}_2$  (0–2 mM). The dashed line indicates the point at which the concentration of hydrogen peroxide overcomes the concentration of TCEP in the buffer.  $\text{H}_2\text{O}_2$  values corrected for the presence of TCEP are shown in red. The panel for WT is the same as shown in Fig. 2D to show comparisons of the WT enzyme with mutants.

nate within the sequence-conserved regulatory domain. To test this, we first examined reduced and oxidized PKG I $\beta$ . PKG I $\beta$  stimulated by cGMP under reducing conditions displayed a cooperative, 86-fold stimulation of activity with a  $K_a$  of 1.21  $\mu\text{M}$  (Table 1 and Fig. S3). When PKG I $\beta$  was oxidized with  $\text{H}_2\text{O}_2$ , a 10-fold increase in basal activity was observed (0.42  $\mu\text{mol}/\text{min} \times \text{mg}$ ) paired with a 1.3-fold decrease in maximal velocity (2.780  $\mu\text{mol}/\text{min} \times \text{mg}$ ), resulting in a reduction of the cGMP-stimulated -fold activation to 6.6. In addition, under oxidizing conditions, the activation constant for PKG I $\beta$  decreased by 1.4-fold ( $K_a = 0.86 \mu\text{M}$ ), and cooperativity was reduced to 1.2. These data suggest that oxidation also affects the activity of the  $\beta$  isoform.

In addition to the interprotomer disulfide bond between Cys-42 and Cys-42', Landgraf *et al.* (11) also confirmed the presence of an intraprotomer disulfide bond between Cys-117 and Cys-195. This disulfide bond has been observed in the crystal structure of the PKG I regulatory domain (PDB code 3SHR) (27). Due to its location in the first cGMP-binding domain (CNB-A), we hypothesized that this disulfide bond may control oxidative activation of PKG I $\alpha$ . To test this, we expressed and purified the PKG I $\alpha$  C117S mutant. Under reducing conditions, C117S<sub>red</sub> had a low basal activity that was similar to that of PKG I $\alpha$  WT<sub>red</sub> (Fig. 3C). Furthermore, activation of C117S<sub>red</sub> with cGMP increased the activity by 26-fold with positive cooperativity ( $n_H = 1.4$ ), resulting in a  $V_{\text{max}}$  of 4.09  $\mu\text{mol}/\text{min} \times \text{mg}$  and a  $K_a$  of 130 nM. In contrast to PKG I $\alpha$  WT, stimulation of C117S<sub>ox</sub> by cGMP resulted in only a slight increase in basal activity and no significant change in its maximal velocity compared with C117S<sub>red</sub> (3.81  $\mu\text{mol}/\text{min} \times \text{mg}$ ). However, the  $K_a$  for cGMP was increased, and the cooperativity showed a slight, but not statistically significant, decrease ( $n_H = 1.2$ ) compared

with C117S<sub>red</sub>. These data suggest that the response to  $\text{H}_2\text{O}_2$  is highly attenuated by introduction of the C117S mutation.

To determine whether oxidative activation depends on disulfide bond formation with Cys-195, we next examined the C195S construct. Under reducing conditions, the overall kinetic profile of C195S<sub>red</sub> was not significantly different from that of WT<sub>red</sub>. However, the basal and maximal activities were slightly elevated, resulting in an overall -fold activation of 10.8 when stimulated with cGMP (Fig. 3D and Table 1). Under oxidizing conditions, we observed kinetics consistent with the WT<sub>ox</sub> phenotype. This included a significant increase in basal activity and a decrease in the maximal velocity, suggesting that oxidation at Cys-195 is not necessary for oxidation-dependent activation.

### Analysis of $K_{Ca}$ 1.1 channel activity during exposure to PKG I $\alpha$

Phosphorylation of the  $K_{Ca}$  1.1 channel by PKG I $\alpha$  has been shown to increase its open probability, resulting in increased  $\text{K}^+$  flux to the extracellular space (5, 33, 34). To examine the effects of both substrate targeting by PKG I $\alpha$  and activation of the channel, we measured  $K_{Ca}$  1.1 channel currents in the inside-out patch-clamp configuration using exogenously applied reduced or oxidized PKG I $\alpha$  constructs (Fig. 4A). Under reducing and cGMP-stimulating conditions, PKG I $\alpha$  WT increased the open probability of the  $K_{Ca}$  1.1 channels by 3.2-fold compared with control patches (+PKG, -cGMP;  $p < 0.001$ ). PKG I $\alpha$  that was pretreated with  $\text{H}_2\text{O}_2$  and then added to the extracellular face of the patch in the absence of cGMP also increased the open probability by 3.1-fold ( $p < 0.02$ ).

Application of C42S<sub>red</sub> under cGMP-saturating conditions did not result in a significant increase in channel open probability compared with the control condition ( $NP_{\text{o(exp)}}$ /

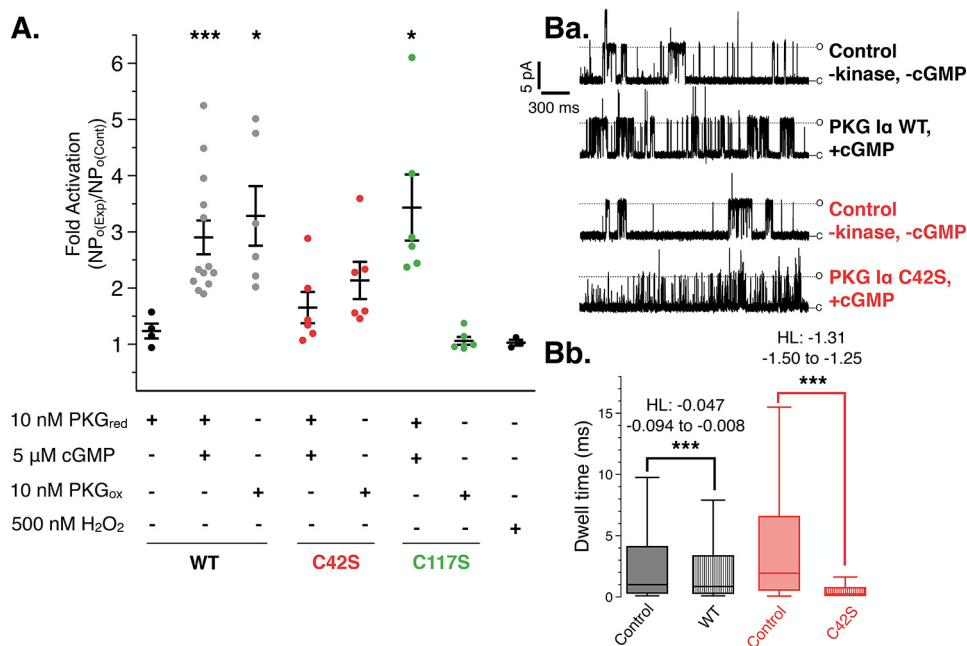


**Figure 4. Stimulation of K<sub>Ca</sub> 1.1 channels with PKG I $\alpha$  constructs under reducing and oxidizing conditions.** *A*, the combined results of single K<sub>Ca</sub> 1.1 recordings exposed to PKG I $\alpha$  constructs under reducing and oxidizing conditions. Individual measurements are represented as a scatter plot overlaid with mean  $\pm$  S.E. (error bars). *p* values represent the comparison against PKG I $\alpha$  under reduced, unstimulated conditions (first lane). *Ba*, representative control (top) and experimental traces of single K<sub>Ca</sub> 1.1 channel openings in excised membrane patches from mouse cerebral artery myocytes under control conditions and when exposed to cGMP activated PKG I $\alpha$  WT and C42S constructs. All measurements were recorded under reducing conditions. *Bb*, analysis of channel open dwell times of K<sub>Ca</sub> 1.1 channels from patches under baseline control ( $-$ PKG,  $-$ cGMP), PKG I $\alpha$  WT<sub>red</sub>-exposed, and C42S<sub>red</sub>-exposed conditions. Whisker boxes, medians bounded by the interquartile ranges. The results of the nonparametric Hodges–Lehmann analyses (HL; coefficient and error) are shown. \*, *p* < 0.02; \*\*\*, *p* < 0.0001.

$NP_{o(\text{baseline})} = 1.4$ ), whereas C42S<sub>ox</sub> resulted in a slightly higher increase in the open probability of the channels to 2.1-fold over baseline. Furthermore, we observed that the channel kinetics in the presence of C42S were altered under these conditions (Fig. 4*Ba*). Examination of the channel dwell times showed that K<sub>Ca</sub> 1.1 patches exposed to cGMP-activated C42S<sub>red</sub> had a shortened mean open dwell time of 1.0 ms compared with baseline (5.8 ms) (Fig. 4*Bb*). However, when PKG I $\alpha$ WT<sub>red</sub> was applied to the patch, we saw a significant but smaller decrease in mean open dwell time (baseline = 4.6 ms and PKG I $\alpha$  = 3.7 ms) (Fig. 4*Bb*). Analysis of median open dwell times also indicated significant decreases (Fig. S4). The comparison of these dwell-time differences by nonparametric Hodges–Lehmann analysis indicated that the change in dwell time in response to kinase addition was greater for C42S than WT PKG I $\alpha$  (Fig. 4*Bb*). To determine whether the change in K<sub>Ca</sub> 1.1 currents caused by C42S depended on activity, channel recordings in the presence of C42S<sub>red</sub> were also measured under symmetrical K<sup>+</sup> in the absence of cGMP and ATP (Fig. S5). The short channel openings (flickers) were observed at both +40 and  $-$ 40 mV, indicating that the effect was independent from C42S activity and membrane polarity.

Finally, application of C117S<sub>red</sub> under cGMP-saturating conditions significantly increased the open probability of the channel compared with the control condition (Fig. 4*A*, *p* < 0.02). However, C117S that was pretreated with H<sub>2</sub>O<sub>2</sub> (C117S<sub>ox</sub>) had no effect on K<sub>Ca</sub> 1.1 channel open probability (*p* = 0.2413). As a control, no effect on channel activity was observed with the addition of 500 nM H<sub>2</sub>O<sub>2</sub>, the concentration that equaled the

maximum final concentration of H<sub>2</sub>O<sub>2</sub> in the bath solution after the addition of PKG I $\alpha$ <sub>ox</sub> constructs.

## Discussion

PKG I $\alpha$  is an essential signaling molecule in the vasculature and can be activated by cGMP or oxidation (10, 35–38). The first study to describe that PKG I $\alpha$  can be constitutively activated by oxidation used cupric cations as the oxidizing agent (11). This activity was found to be blocked by iodoacetamide, which indicated involvement of cysteine residues in this mechanism. Moreover, three possible disulfide bonds were identified by nonreducing SDS-PAGE and Edmann degradation: an interprotomer disulfide bond between Cys-42 and Cys-42', an intra-protomer disulfide bond between Cys-117 and Cys-195, and an intraprotomer disulfide bond between Cys-312 and Cys-518. Of the three, the last disulfide bond could not be definitively confirmed, and no other functions have been ascribed to the remaining cysteine residues.

Previous analyses of PKG I isoforms determined that PKG I $\alpha$ , but not PKG I $\beta$ , exhibits sensitivity to oxidation (10, 12). Thus, it was concluded that Cys-42, the only cysteine residue unique to PKG I $\alpha$ , must be the primary regulator of oxidation-dependent activation (10). Moreover, formation of this interprotomer disulfide bond between Cys-42 and Cys-42' of the opposing protomer was found to correlate with a vasodilatory response in isolated perfused rat hearts (10). These observations helped to cement oxidation as an additional mechanism by which PKG I $\alpha$  can be activated. Despite an abundance of data ascribing physiological importance to the formation of the interprotomer

## Oxidation-dependent activation of PKG I $\alpha$ Cys-117

disulfide bond between Cys-42 and Cys-42', the structural and biochemical underpinnings of how this disulfide bond would activate PKG I $\alpha$  remain unclear. Thus, we sought to expand upon these initial observations to more thoroughly understand the mechanism of oxidation-dependent activation in PKG I $\alpha$ . Signaling by PKG I isoforms is mediated by both substrate targeting and activation (6, 23, 24, 26, 36, 39–42). More importantly, they can be considered independent because disruption of either facet alters PKG I signaling pathways (23–26). In this study, we sought to separate these aspects of PKG I signaling to better understand how oxidation may regulate each of these processes. The use of a synthetic peptide substrate allowed for a thorough examination of the effect of oxidation that was independent from substrate targeting through the dimerization domain.

Under reducing conditions, the cGMP-dependent activation characteristics of PKG I $\alpha$  WT were consistent with previously reported values (Fig. 2C) (29, 30). Furthermore, its preincubation with H<sub>2</sub>O<sub>2</sub> induced interprotomer disulfide bond formation (Fig. 2D) (10, 11, 43). We observed that exposure of WT enzyme to 500  $\mu$ M H<sub>2</sub>O<sub>2</sub> for 30 min at 24 °C resulted in the greatest amount of constitutive activation, determined by an increase in basal activity and a corresponding decrease in cGMP-dependent activation (Fig. 2B). Although this concentration of H<sub>2</sub>O<sub>2</sub> is significantly higher than what has been implemented in prior studies, we sought to measure the H<sub>2</sub>O<sub>2</sub> concentration dependence on PKG I $\alpha$  activity in a way similar to that used by Landgraf *et al.* (10–12, 43).

### Characterization of C42S provides insight into rodent models of oxidation-dependent activation of PKG I $\alpha$

When cGMP-dependent activation of C42S was examined under reducing conditions, we observed that the presence of the serine mutant significantly altered enzyme activity (Fig. 3A). This overall shift in efficacy and potency (3-fold) culminated in a 90% reduction in activity for C42S under cGMP concentrations near the  $K_a$  for PKG I $\alpha$  WT. Even under maximum cGMP concentrations typically observed in smooth muscle cells (1–2  $\mu$ M), C42S exhibited only about 30% of the maximal activity of PKG I $\alpha$  WT (Fig. 3A) (44). Based upon these results, we conclude that the C42S mutant retains sensitivity to oxidation, and, unlike the WT enzyme, the reduced form of C42S displays a significantly altered kinetic profile toward the synthetic peptide substrate used in the *in vitro* phosphotransferase assays. In agreement with previous results, C42S did not form an interprotomer disulfide bond in the presence of H<sub>2</sub>O<sub>2</sub> (Fig. 3E) (10, 43). These results are consistent with a recent study that found that the reduced form of C42S exhibited a 5-fold shift in its activation constant for cGMP. Taken together, these results suggest that the interprotomer disulfide bond does not mediate the oxidative phenotype but does offer an explanation of the detrimental physiological phenotypes associated with this mutation.

Previous studies investigating the physiological effects of the interprotomer disulfide bond used a PKG I $\alpha$  C42S knock-in mouse model (14). These mice were found to be hypertensive compared with littermate controls. Based upon our kinetic analyses of PKG I $\alpha$  C42S, we suggest that this phenotype may

result from the compromised kinetic profile of the enzyme rather than an inability to be activated by oxidation. This conclusion is further substantiated by the effects of PKG I $\alpha$  constructs on K<sub>Ca</sub> 1.1 channel activity (Fig. 4A). The similarities in channel responses between the oxidizing and reducing conditions suggest that substrate targeting of PKG through its dimerization domain to K<sub>Ca</sub> 1.1 is not compromised by formation of the interprotomer disulfide bond between Cys-42 and Cys-42' in the dimerization domain.

A comparison of K<sub>Ca</sub> 1.1 channel characteristics subjected to either C42S or WT uncovered the presence of channel “flickers” for patches treated with C42S and an overall increase in the number of channel opening events over an equivalent time period (Fig. 4Bb and Figs. S4 and S5). Moreover, the K<sub>Ca</sub> 1.1 channel flickers were observed for all patches exposed to C42S (with or without cGMP and under oxidizing conditions) (Fig. 4Bb and Figs. S4 and S5). Within this context, a study examining pressure-induced constriction of third order mesentery arteries expressing C42S observed that application of the K<sub>Ca</sub> 1.1 channel blocker, paxilline, did not induce vessel constriction (13). In light of the modified K<sub>Ca</sub> 1.1 channel characteristics that were observed herein with C42S, the mutation may possess hitherto unknown properties, such as unique interactions with the channel pore or altered targeting to other PKG I $\alpha$  substrates.

The effects of disrupted substrate targeting have been observed previously for a mutant leucine zipper knock-in mouse model in which the leucine residues in the dimerization domain were mutated to alanine residues. This mutant was unable to phosphorylate the myosin-binding subunit and the Ras homolog A (RhoA), despite retaining its sensitivity to cGMP and ability to phosphorylate the synthetic substrate, BPDEtide (23). Furthermore, these mice, like the C42S knock-in model, were also hypertensive. Since substrate targeting through the dimerization domain and activation are both required for phosphorylation of substrates by PKG I $\alpha$ , we suggest that either explanation is possible.

### C117S drives constitutive activation of PKG I $\alpha$ by oxidation

To test our hypothesis that the oxidative phenotype is driven by residues that lie outside of the N terminus, we used the PKG I $\alpha$  truncation construct,  $\Delta$ 53 (30). Similar to C42S,  $\Delta$ 53 does not form an interprotomer disulfide bond (Fig. 3E). However, oxidation had the most pronounced effect on this construct, as indicated by the complete insensitivity to cGMP. These results corroborate the C42S data and overwhelmingly demonstrate that the interprotomer disulfide bond is not required for oxidation-induced activation.

Finally, we tested the contribution of the intraprotomer disulfide bond that has been shown to form between Cys-117 and Cys-195 in the cGMP-A domain (11, 27). We observed that oxidized C117S exhibited only a modest increase in basal activity and no reduction in maximal velocity compared with its reduced form and that of WT (Fig. 3C). We also consistently observed robust activation by cGMP under oxidizing conditions, indicating that the C117S mutation nearly abolishes the oxidative phenotype; these results are further corroborated by the inside-out patching experiments. Finally, with the C195S

## Oxidation-dependent activation of PKG I $\alpha$ Cys-117

mutant, we observed an activation profile similar to that of WT under both reducing and oxidizing conditions. Thus, we conclude that Cys-117 plays a unique role in mediating oxidative activation of PKG I $\alpha$  *in vitro*.

The initial observation that PKG I $\alpha$  and I $\beta$  exhibit differing responses to H<sub>2</sub>O<sub>2</sub> has predominantly focused the field on Cys-42, the cysteine residue specific to the I $\alpha$  isoform. However, the results described herein indicate that the oxidative phenotype is controlled by Cys-117 in the cyclic nucleotide binding domain-A (CBD-A). PKG I $\alpha$  and I $\beta$  are 100% identical in this region, and the residue analogous to Cys-117 in PKG I $\beta$  is Cys-132. Thus, we examined PKG I $\beta$  and found that oxidation had a significant impact on its maximal velocity that was similar to the effect on PKG I $\alpha$ . However, only a slight increase in basal activity was observed. Our results are consistent with a previous study that focused solely on activation of PKG I $\beta$  with H<sub>2</sub>O<sub>2</sub> in the absence of cGMP (10) and indicate that examination of the full cGMP-dependent activation profile is necessary to observe the full effects of oxidation on PKG I $\beta$  activity. Differences in PKG I $\alpha$  and I $\beta$  (cGMP-dependent activation profiles and targeting to substrates) are attributable to their distinct N termini (35, 45, 46). We propose that their N termini also dictate their oxidation-dependent phenotypes and suggest a model by which this could occur.

### A model for oxidation-driven activation in PKG I $\alpha$ and considerations for pathophysiological conditions

The results obtained using the PKG I $\alpha$  mutant constructs suggest that Cys-117 is necessary and sufficient to stimulate constitutive activation of PKG I $\alpha$ . Under mild oxidizing conditions, Cys-117 and Cys-195 would form sulfenic acid intermediates, which can be reduced to the free thiol or condensed to a disulfide form (Fig. 5A). The fact that no discernible structural changes have been observed between the reduced and disulfide-bonded forms of CBD-A suggests that the site maintains an inactive conformation in both states and that disulfide bond formation between Cys-117 and Cys-195 likely mitigates oxidative activation (19, 27, 47). As determined by this study and Landgraf *et al.* (11), increasing the concentrations of oxidant causes the  $V_{\max}$  of the kinase to decay, resulting in a rise in constitutive activity. The reversibility of the oxidized phenotype measured previously was determined at concentrations that did not affect the  $V_{\max}$  (10, 11). This suggests that formation of sulfenic and sulfonic acid species at Cys-117 may drive the cGMP insensitivity that is observed at high concentrations of H<sub>2</sub>O<sub>2</sub>.

In support of this model, we observed cysteine modifications on tryptic peptides of the oxidized form of PKG I $\alpha$  by MS and found that Cys-117 can adopt disulfide and sulfonic acid species, whereas Cys-195 can only adopt a disulfide-bound form (Table 2). This suggests that the higher-order sulfur acids occur preferentially on Cys-117 over Cys-195. Consequently, it is equally probable for the oxidation of Cys-117 to higher-order sulfur acids to proceed with or without the disulfide-bound intermediary form. We also found that Cys-42 can adopt disulfide, sulfenic, and sulfonic acid forms in the oxidized state, which further reinforce that, despite the presence of higher-order sulfur acid species in the N terminus, their effects on

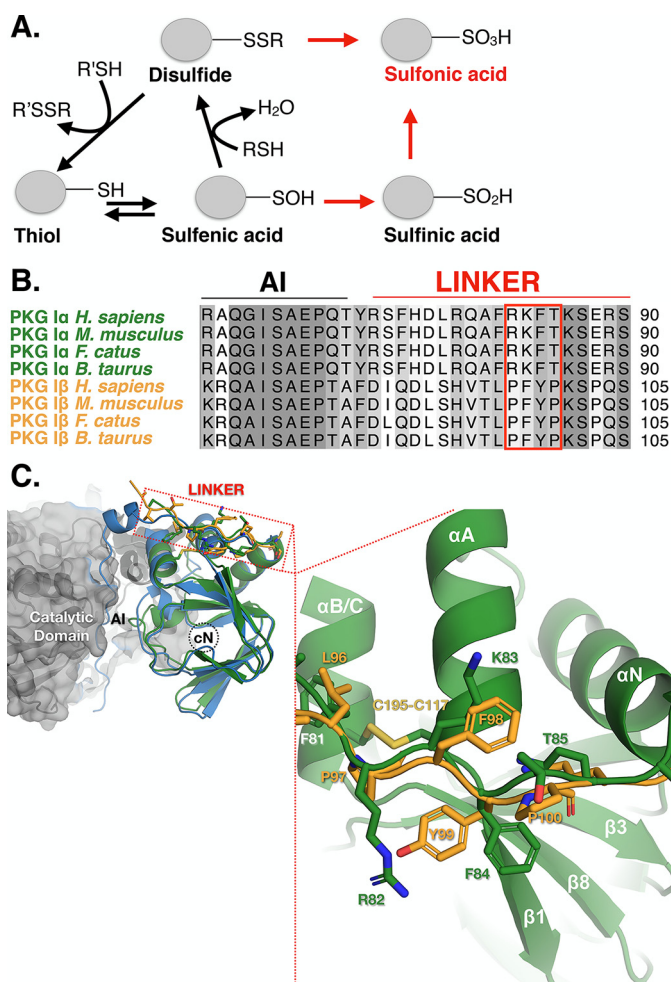


**Figure 5. Model of the oxidation-dependent activation of PKG I $\alpha$ .** A, cysteine residues can be oxidized to multiple states, which proceed through a sulfenic acid intermediate. When in proximity to a free thiol, sulfenic acids can be condensed to a disulfide. Further oxidation of sulfenic acids results in the irreversible sulfenic and sulfonic acid forms. The sulfonic acid form can also be reached via a thiosulfinate intermediate. B, sequence alignment of mammalian PKG I $\alpha$  (green) and I $\beta$  (gold) isoforms denoting the autoinhibitory (AI) domain and linker region. The segment within the linker region that is in close proximity to Cys-117 is boxed in red. C, structural alignment of the PKG I $\alpha$  (green; PDB code 3SHR) and I $\beta$  (yellow; PDB code 3OD0) A-sites superimposed with the RI $\alpha$ :C holoenzyme of PKA (RI $\alpha$  (blue) and C (gray); PDB code 2QCS). The boxed region indicates the location of the linker region of PKG I $\alpha$  and I $\beta$  with their corresponding residues within close proximity to Cys-117.

enzymatic activity are limited. Based upon the available crystal structures and these data, we propose a model of constitutive, cGMP-independent activation of PKG I $\alpha$  that is driven through oxidation of Cys-117 to either the sulfenic, sulfenic, or sulfonic acid intermediates. However, due to its exposure to solvent, it is likely that the interprotomer disulfide bond at Cys-42 may act as a buffering mechanism to preclude the formation of sulfur acid species at Cys-117.

A sequence alignment of PKG I $\alpha$  and I $\beta$  paired with a structural alignment of the PKG I CBD-A and the PKA RI $\alpha$ :C holoenzyme shows that Cys-117 is oriented proximal to the linker region that connects the autoinhibitory domain and CBD-A. This region contains very low sequence identity (~6%) between I $\alpha$  and I $\beta$  (Fig. 5B). We propose that the presence of the basic residues (Arg-82 and Lys-83) within the linker region of PKG I $\alpha$  may form hydrogen bonds or a salt bridge with the

## Oxidation-dependent activation of PKG I $\alpha$ Cys-117

**Table 2**

Identification of cysteine-containing peptides from oxidized PKG I $\alpha$

Cysteine	Sequence with modifications <sup>a</sup>	z <sup>+</sup>	Theoretical m/z (monoisotopic)	Observed m/z (monoisotopic)	Concentration	Retention time
					ppm	min
Cys-42	K ↓ C <sup>@</sup> QSVLPVPSTHIGPR ↓ T	2	819.917	819.917	0.00	37.88
	K ↓ C <sup>@</sup> QSVLPVPSTHIGPR ↓ T	2	811.920	811.921	1.23	37.96
	K ↓ C <sup>^</sup> QSVLPVPSTHIGPR ↓ T	2	824.435	824.437	2.42	34.34
	K ↓ C <sup>^</sup> QSVLPVPSTHIGPR ↓ T	2	844.433	844.435	2.37	40.13
Cys-117	K ↓ NLELSQIQEIVDC <sup>@</sup> M*YPVEYGK ↓ D	3	845.726	845.724	-2.36	58.92
	K ↓ NLELSQIQEIVDC <sup>^</sup> M*YPVEYGK ↓ D	3	848.738	848.739	1.17	58.25
	K ↓ NLELSQIQEIVDC <sup>~</sup> M*YPVEYGK ↓ D	3	862.070	862.069	1.15	58.89
Cys-195	R ↓ QC <sup>-</sup> FQTIMMR ↓ T	2	627.775	627.776	1.59	24.48
	R ↓ QC <sup>-</sup> FQTIM*MR ↓ T	2	635.773	635.772	1.57	30.43
	R ↓ QC <sup>-</sup> FQTIM*M*R ↓ T	2	643.770	643.771	1.55	34.03

<sup>a</sup> Modifications were as follows: \*, oxidation; #, sulfinic acid; @, sulfonic acid; ^, iodoacetamide (free thiol, previously disulfide-bound); ~, maleimide (free thiol).

sulfur acid forms of Cys-117 (Fig. 5C). In comparison, this region in PKG I $\beta$  contains hydrophobic residues (Pro-97 and Phe-98) at the equivalent positions. In this model, we propose that an interaction between the acid form of Cys-117 and the linker region in PKG I $\alpha$  could alter the conformation of the linker to release the autoinhibitory segment from the catalytic domain, resulting in constitutive activation. We further propose that our model may provide an explanation of the differing responses to oxidation between the two type I isoforms.

PKG I $\alpha$  has been reported to be activated by cGMP-independent mechanisms in both physiological and pathophysiological states (10, 11, 12, 15, 48). Oxidizing agents, particularly H<sub>2</sub>O<sub>2</sub>, have been suggested to play important roles in a number of conditions associated with vascular remodeling, including angiogenesis, atherosclerosis, and hypertension (16–22, 49). Typically, H<sub>2</sub>O<sub>2</sub> concentrations in mammalian cells are estimated to average between 1 and 700 nM (50). However, local levels caused by bursts in H<sub>2</sub>O<sub>2</sub> production are suggested to greatly exceed the average value and depend on the distance from the source and local concentrations of antioxidants, such as catalase, GSH peroxidases, and thioredoxin reductases. A recently developed H<sub>2</sub>O<sub>2</sub> sensor (HyPer-Tau) coupled with superresolution microscopy suggested that local bursts of hydrogen peroxide can reach 50–100  $\mu$ M (49). In addition, the presence of peroxiredoxin hubs has been suggested to neutralize ~90% of the H<sub>2</sub>O<sub>2</sub> produced in cells, which would further limit the effect of H<sub>2</sub>O<sub>2</sub> to specific microdomains (51). The data presented herein indicate that constitutive PKG I $\alpha$  activation via oxidation does not occur until 500  $\mu$ M and involves long-lived exposure to the oxidant. Thus, this mechanism would be specifically relevant to PKG I $\alpha$  anchored near hydrogen peroxide sources or under pathophysiological conditions associated with high global intracellular concentrations of hydrogen peroxide.

### Experimental procedures

#### Site-directed mutagenesis of WT PKG I $\alpha$

WT PKG I $\alpha$  and PKG I $\beta$  from *Bos taurus* (NCBI entries NP\_776861.1 and CAA70155.1) were cloned into pFAST Bac HTA as described previously (34, 49). The PKG I $\alpha$  construct was used as a template for site-directed mutagenesis to produce the following mutants: PKG I $\alpha$  C42S, PKG I $\alpha$  C42A, PKG I $\alpha$  C117S, and PKG I $\alpha$  C195S. The forward and reverse primers used to generate these constructs were synthesized as follows:

C42S, 5'-AAG AGG AAA CTC CAT AAA AGC CAG TCA GTG-3' (sense) and 5'-GGG CAG CAC TGA CTG GCT TTT ATG GAG-3' (antisense); C42A, 5'-AAG AGG AAA CTC CAT AAA GCC CAG TCA GTG-3' (sense) and 5'-GGC AGC ACT GAC TGG GCT TTA TGG-3' (antisense); C117S, 5'-ATC CAA GAG ATT GTG GAT AGT ATG TAC CCA GTG-3' (sense) and 5'-GCC GTA CTC CAC TGG GTA CAT ACA ATC CAC AAT-3' (antisense); C195S, 5'-GCC ATT GAC CGA CAA TCT TTT CAG ACG-3' (sense) and 5'-CCT CAT TAT CGT CTG AAA AGA TTG TCG-3' (antisense). All site-directed mutagenesis experiments were carried out using the QuikChange (Stratagene) method.

#### Expression and purification of PKG I constructs

PKG I $\alpha$  and I $\beta$  WT, PKG I $\alpha$  mutant constructs, and PKG I $\alpha$   $\Delta$ 53 were expressed in Sf9 cells using the Bac-to-Bac Baculovirus Expression System as described previously (29, 30). Constructs were purified from Sf9 cell pellets by nickel immobilized metal ion affinity chromatography using either prepacked (5 ml; Bio-Rad) or hand-packed nickel-nitrilotriacetic acid columns. Protein purified for use in inside-out patch clamp experiments was prepared without the N-terminal hexahistidine tag, by incubation with His-tagged tobacco etch virus (TEV) protease at a 1:20 mass ratio (TEV/PKG) during the first dialysis step (50 mM MES, 300 mM NaCl, 1 mM TCEP, pH 6.9, 4 °C, 16 h). TEV and the histidine tag were subtracted from the cleaved protein by flowing over a nickel immobilized metal ion affinity chromatography column. The resulting flow-through containing PKG I was concentrated to 1 mg/ml and dialyzed against 1 liter of 50 mM MES, 150 mM NaCl, 1 mM TCEP, 10% glycerol, pH 6.9, at 4 °C. The resulting protein solution was divided into 20–100- $\mu$ l aliquots, flash-frozen in liquid nitrogen, and stored at -80 °C.

#### Determination of H<sub>2</sub>O<sub>2</sub> concentration

The primary H<sub>2</sub>O<sub>2</sub> stock (stored at 4 °C) was measured by absorption spectroscopy at  $\lambda = 240$  nm (43.6 M<sup>-1</sup> cm<sup>-1</sup>) to determine its concentration (31, 32). Fresh dilutions were prepared daily from the stock for use in experiments.

#### Measurement of interprotomer disulfide bond formation by SDS-PAGE

PKG I constructs were buffer-exchanged (1–4 times) into 50 mM MES, 150 mM NaCl, 1 mM TCEP, pH 6.9, using 3000



MWCO ultracentrifugal filter units (Amicon) to remove glycerol (to <1%) in the storage buffer. PKG concentration was determined by measuring the absorbance at 280 nm (equal to  $81,250 \text{ M}^{-1} \text{ cm}^{-1}$  as calculated by ProtParam (51)). All constructs were adjusted to 1 mg/ml (13.1  $\mu\text{M}$  of monomer), and PKG (3.6  $\mu\text{l}$ ) was added to 1.4  $\mu\text{l}$  of  $\text{H}_2\text{O}_2$  (freshly prepared  $10\times$  stocks that ranged from 0 to 50 mM) and 9  $\mu\text{l}$  of 50 mM MES, 150 mM NaCl, pH 6.9 (in the absence of reducing agent) ( $14\times$  reactions). Reactions proceeded for 30 min at 24 °C and were subsequently quenched by the addition of 2  $\mu\text{l}$  of 1 M maleimide (10% DMSO stock) and 4  $\mu\text{l}$  of  $5\times$  SDS-loading buffer without reducing agent. Samples were boiled for 2 min at 95 °C and separated by SDS-PAGE using 4–20% TGX gradient gels (Bio-Rad). The resulting gels were stained with InstantBlue Protein Stain (Expedeon) and imaged using an Odyssey IR Scanner (LI-COR) at 700 nm. Bands were selected and quantified in the Image Studio Software (LI-COR) using intensity analysis relative to background. The background was subtracted by implementing the mean intensity background subtraction method. Images were exported as 600 DPI gray-scale TIFF files for use as figures. Data analysis was achieved using Prism version 7 (GraphPad).

#### *In vitro* phosphotransferase assays

Activation of reduced PKG I constructs by cGMP (BioLog) was assessed by measuring phosphorylation of a synthetic peptide substrate (W15, TQAKRKKSLAMA) with [ $\gamma$ - $^{32}\text{P}$ ]ATP as described previously (35). To measure the cGMP-dependent activation under oxidized conditions, PKG I constructs were preincubated with 500  $\mu\text{M}$   $\text{H}_2\text{O}_2$  in 50 mM MES, pH 6.9, for 30 min at 24 °C. Under these conditions, the 1 mM TCEP in the PKG storage buffer was diluted to a final concentration of 500 nM. Oxidized PKG I was then added to the other reaction components (in the absence of reducing agent) to initiate the reactions. All subsequent steps were performed following the same procedure as the reduced PKG conditions.

#### Measurement of $K_{\text{Ca}}$ 1.1 activation by inside-out patch clamp of vascular smooth muscle cells

Male C57BL/6 mice (3–6 months old) were euthanized using procedures approved by the institutional animal care and use committee at the University of Vermont and performed in accordance with the National Institutes of Health policy on the care and use of laboratory animals. The anterior and posterior pial and superior cerebellar arteries were isolated and cleaned of connective tissue. The arteries were then incubated at 37 °C in dissociation solution (55 mM NaCl, 80 mM sodium glutamate, 6 mM KCl, 2 mM  $\text{MgCl}_2$ , 10 mM glucose, 10 mM HEPES, pH 7.3) containing 0.5 units/ml papain (Worthington) and 1 mg/ml dithioerythritol for 12 min followed by a 10-min incubation in dissociation solution containing 1 mg/ml collagenase (Worthington Type 4). Arteries were then removed and placed back in the isolation solution without enzymes for an additional 10 min before trituration with a polished Pasteur pipette to yield single smooth muscle cells. Cells were left to stick to the glass coverslip in the experiment chamber for 10 min before use.

Membrane patches were pulled from the isolated vascular smooth muscle cells to achieve the inside-out configuration

and contained 2–10  $K_{\text{Ca}}$  1.1 channels each.  $K_{\text{Ca}}$  1.1 single-channel currents were recorded under the following conditions. The pipette solution contained 6 mM KCl, 134 mM NaCl, 1 mM  $\text{MgCl}_2$ , 10 mM HEPES, pH 7.4 (NaOH); the bathing solution contained 135 mM KCl, 2 mM  $\text{MgCl}_2$ , 1.4787 mM  $\text{CaCl}_2$ , 2 mM EGTA, 10 mM HEPES, adjusted to pH 7.2 with 14.85 mM KOH. The concentration of free  $\text{Ca}^{2+}$  on the intracellular face was calculated to be 500 nM using the online software WEBMAXC Standard (<https://web.stanford.edu/~cpatton/webmaxcS.htm>;<sup>4</sup> Stanford University, Stanford, CA). Single  $K_{\text{Ca}}$  1.1 channel recordings were obtained at room temperature (25 °C) for at least 5 min at 0 mV and using an Axopatch 200 B amplifier coupled to a Digidata 1332A digital-to-analog converter. Currents were filtered at 2 kHz, digitized at 20 kHz using pCLAMP version 9.2 software (Axon Instruments), and then analyzed with Clampfit version 9.2 using the half-amplitude threshold method. The baseline activity was recorded for at least 20 min to ensure patch stability. The experimental condition was measured after the addition of 100  $\mu\text{M}$  ATP and either reduced, inactive PKG I $\alpha$  (no cGMP added), PKG I $\alpha$  constructs activated with 5  $\mu\text{M}$  cGMP, or PKG I $\alpha$  constructs activated with 500  $\mu\text{M}$   $\text{H}_2\text{O}_2$ . For the oxidized condition, PKG I $\alpha$  constructs were first buffer-exchanged into 50 mM MES, 150 mM NaCl, 1 mM TCEP, pH 6.9, using MWCO 3000 ultracentrifugal filter units (Amicon) to remove the glycerol (to <1%) in the storage buffer. Assuming a 1:1 negation of TCEP with  $\text{H}_2\text{O}_2$  (31, 32), PKG I $\alpha$  constructs were oxidized with a final concentration of 500  $\mu\text{M}$   $\text{H}_2\text{O}_2$  at 24 °C for 30 min before use in patch clamp experiments. The addition of PKG I $\alpha$  constructs to the bath solution (5 ml) resulted in a final concentration of  $\text{H}_2\text{O}_2$  that was less than 500 nM. The -fold activation was determined as the open probability of the channels ( $NP_o$ ) during the experimental condition/ $NP_o$  at baseline. The -fold activations of the experimental conditions were compared with the control condition (reduced PKG I $\alpha$ , 0 cGMP) using unpaired *t* tests with Welch's correction in Prism version 7 (GraphPad).  $K_{\text{Ca}}$  1.1 channel open times within 5-min windows were measured from full-length PKG I $\alpha$ , C42S, and their respective baseline recordings using Clampfit version 9.2. The mean channel open dwell times ( $\tau$ ) and interquartile ranges were calculated using the Mann–Whitney test, and the differences between the baseline control and experimental dwell times were compared using a non-parametric Hodges–Lehmann analysis in Prism version 7 (GraphPad). Channel recordings examining the effects of C42S on  $K_{\text{Ca}}$  1.1 were run under symmetrical  $\text{K}^+$ , 5  $\mu\text{M}$   $\text{Ca}^{2+}$  in the presence of reduced C42S (–cGMP) at +40, 0, and –40 mV.

#### Sequence alignments

Sequences for PKG I $\alpha$  and I $\beta$  were downloaded from the National Center for Biotechnology Information (NCBI) database, and a multiple-sequence alignment was performed with JalView Desktop using CLUSTAL-O (52, 53). The following accession numbers were used: *Homo sapiens*, I $\alpha$ -NP\_001091982.1 and I $\beta$ -NP\_006249.1; *Mus musculus*, I $\alpha$ -NP\_001013855.1 and I $\beta$ -NP\_035290.1; *Felis catus*, I $\alpha$ -XP\_

<sup>4</sup> Please note that the JBC is not responsible for the long-term archiving and maintenance of this site or any other third party hosted site.

## Oxidation-dependent activation of PKG I $\alpha$ Cys-117

023096056.1 and I $\beta$ -XP\_023096055.1; *B. taurus*, I $\alpha$ -NP\_776861.1 and I $\beta$ -CAA70155.1.

### Mass spectrometry

For MS analysis to identify the cysteine oxidation states induced by H<sub>2</sub>O<sub>2</sub>, His-tagged PKG I $\alpha$  was thawed on ice and buffer-exchanged into 50 mM MES, 300 mM NaCl, 1 mM TCEP (pH 6.9) (Buffer 1) using a 10,000 MWCO centrifugal concentrator (Millipore). Samples were oxidized with a final concentration of 500  $\mu$ M H<sub>2</sub>O<sub>2</sub> for 30 min at room temperature and then buffer-exchanged three times into 50 mM MES, 300 mM NaCl (pH 6.9) (Buffer 2). Dimedone (200 mM stock in 10% DMSO) was added to a final concentration of 20 mM to the reduced and oxidized samples and incubated for 20 min at room temperature. Excess dimedone was removed by buffer exchange by centrifugal concentrator into Buffer 2. Maleimide (200 mM in double-distilled H<sub>2</sub>O) was added to samples at a final concentration of 20 mM, incubated at 24 °C for 20 min, and then removed by buffer exchange as described above. Samples were centrifuged at  $\sim$ 14,500  $\times$  *g* to remove any protein aggregates, and the supernatants were transferred to fresh tubes. TCEP was added at a final concentration of 1 mM and incubated for 20 min at room temperature. Iodoacetamide (200 mM stock in double-distilled H<sub>2</sub>O) was added to the samples at a final concentration of 20 mM and incubated at 24 °C for 20 min. Samples were buffer-exchanged five times in Buffer 1 to ensure removal of the cysteine-modifying agents and digested with trypsin overnight at 37 °C. Tryptic peptides were flash-frozen in liquid nitrogen and stored at  $-80$  °C pending analysis.

ZipTip pipette tips (Merck Millipore) were used to desalt the tryptic peptide samples by first activating with 100% acetonitrile (MeCN) and equilibrated in 0.1% TFA before introduction of tryptic peptides. Bound peptides were washed in 0.1% TFA and eluted with 0.1% TFA in 50% MeCN and dried in a Speed-Vac. Peptides were resuspended in Solvent A (2.5% MeCN, 0.15% formic acid) and separated via HPLC using the Easy n-LC 1200 system before MS/MS analysis on the Q Exactive Plus mass spectrometer fitted with a Nanospray Flex ion source and supplied with Thermo Xcalibur version 4.0 software (Thermo Fisher Scientific). Chromatography columns (15 cm  $\times$  100  $\mu$ m) were packed in-house with 2.7- $\mu$ m C18 packing material (Bruker, Halo, pore size = 90 Å). Peptides were eluted using a 0–50% gradient of Solvent B (80% MeCN, 0.15% formic acid) over 60 min and electrosprayed into the mass spectrometer. This gradient was followed by 10 min at 100% Solvent B before a 15-min equilibration in 100% Solvent A. The precursor scan (scan range = 360–1700 *m/z*, resolution =  $7.0 \times 10^4$ , automatic gain control =  $1.0 \times 10^6$ , maximum ion injection time = 100 ms) was followed by 10 collision-induced dissociation tandem mass spectra for a top 10 approach. Collision-induced dissociation spectra were acquired for the top 10 ions in the precursor scan (resolution =  $3.5 \times 10^4$ , automatic gain control =  $5.0 \times 10^4$ , maximum ion injection time = 50 ms, isolation window =  $\pm$ 1.6 *m/z*, collision energy = 26 eV).

Raw spectra were searched for matches within the forward and reverse sequence of the hexahistidine-tagged PKG I $\alpha$  using SEQUEST, either requiring tryptic peptides or with no enzyme specified, permitting the denoted modifications with a mass

tolerance of 4 ppm. For the SEQUEST search requiring tryptic peptides, cross-correlation (XCORR) scores were filtered to include scores that met the following criteria: for *z* = +1, XCORR 1.8; for *z* = +2, XCORR 2.0; for *z* = +3, XCORR 2.2; for *z* = +4, XCORR 2.4; for *z* = +5, XCORR 2.6.

---

*Author contributions*—J. L. S., T. M. M., and W. R. D. conceived of and designed the experiments. J. L. S. and A. D. B., and A. M. S. performed experiments. J. L. S., T. M. M., and W. R. D. wrote the manuscript with contributions from A. D. B., M. T. N., A. M. S., and B. A. B.

---

*Acknowledgments*—We thank Werner Tegge (Helmholtz Centre for Infection Research (HZI), Braunschweig, Germany) for synthesizing the W15 peptide substrate used in the phosphotransferase assays. Mass spectrometry was supported by the Vermont Genetics Network through National Institutes of Health (NIH) Grant 8P20GM103449 from the INBRE program of NIGMS. SDS-PAGE experiments were imaged with support from NIH Grants 5 P30 RR032135 from the COBRE Program of the National Center for Research Resources and 8 P30 GM103498 from NIGMS. We also thank the Hondal Laboratory at the University of Vermont for helpful discussions and use of resources.

---

### References

1. Friebe, A., and Koesling, D. (2003) Regulation of nitric oxide-sensitive guanylyl cyclase. *Circ. Res.* **93**, 96–105 [CrossRef Medline](#)
2. Hofmann, F., Bernhard, D., Lukowski, R., and Weinmeister, P. (2009) cGMP regulated protein kinases (cgk). *Handb. Exp. Pharmacol.*, 137–162 [CrossRef Medline](#)
3. Fukao, M., Mason, H. S., Britton, F. C., Kenyon, J. L., Horowitz, B., and Keef, K. D. (1999) Cyclic GMP-dependent protein kinase activates cloned bkca channels expressed in mammalian cells by direct phosphorylation at serine 1072. *J. Biol. Chem.* **274**, 10927–10935 [CrossRef Medline](#)
4. Sausbier, M., Arntz, C., Bucurenciu, I., Zhao, H., Zhou, X. B., Sausbier, U., Feil, S., Kamm, S., Essin, K., Sailer, C. A., Abdullah, U., Krippeit-Drews, P., Feil, R., Hofmann, F., Knaus, H. G., *et al.* (2005) Elevated blood pressure linked to primary hyperaldosteronism and impaired vasodilation in bk channel-deficient mice. *Circulation* **112**, 60–68 [CrossRef Medline](#)
5. Schubert, R., and Nelson, M. T. (2001) Protein kinases: tuners of the BKCa channel in smooth muscle. *Trends Pharmacol. Sci.* **22**, 505–512 [CrossRef Medline](#)
6. Kato, M., Blanton, R., Wang, G. R., Judson, T. J., Abe, Y., Myoishi, M., Karas, R. H., and Mendelsohn, M. E. (2012) Direct binding and regulation of rhoa protein by cyclic GMP-dependent protein kinase  $\alpha$ . *J. Biol. Chem.* **287**, 41342–41351 [CrossRef Medline](#)
7. Sun, X., Kaltenbronn, K. M., Steinberg, T. H., and Blumer, K. J. (2005) Rgs2 is a mediator of nitric oxide action on blood pressure and vasoconstrictor signaling. *Mol. Pharmacol.* **67**, 631–639 [Medline](#)
8. Yuen, S., Ogut, O., and Brozovich, F. V. (2011) Mypt1 protein isoforms are differentially phosphorylated by protein kinase G. *J. Biol. Chem.* **286**, 37274–37279 [CrossRef Medline](#)
9. Yuen, S. L., Ogut, O., and Brozovich, F. V. (2014) Differential phosphorylation of lz+ /lz- mypt1 isoforms regulates mlc phosphatase activity. *Arch. Biochem. Biophys.* **562**, 37–42 [CrossRef Medline](#)
10. Burgoyne, J. R., Madhani, M., Cuello, F., Charles, R. L., Brennan, J. P., Schröder, E., Browning, D. D., and Eaton, P. (2007) Cysteine redox sensor in ptkga enables oxidant-induced activation. *Science* **317**, 1393–1397 [CrossRef Medline](#)
11. Landgraf, W., Regulla, S., Meyer, H. E., and Hofmann, F. (1991) Oxidation of cysteines activates cGMP-dependent protein kinase. *J. Biol. Chem.* **266**, 16305–16311 [Medline](#)
12. Müller, P. M., Gnügge, R., Dhayade, S., Thunemann, M., Krippeit-Drews, P., Drews, G., and Feil, R. (2012) H<sub>2</sub>O<sub>2</sub> lowers the cytosolic Ca<sup>2+</sup> concen-

- tration via activation of cGMP-dependent protein kinase  $\alpha$ . *Free Radic. Biol. Med.* **53**, 1574–1583 [CrossRef Medline](#)
13. Khavandi, K., Baylie, R. A., Sugden, S. A., Ahmed, M., Csato, V., Eaton, P., Hill-Eubanks, D. C., Bonev, A. D., Nelson, M. T., and Greenstein, A. S. (2016) Pressure-induced oxidative activation of PKG enables vasoregulation by Ca<sup>2+</sup> sparks and BK channels. *Sci. Signal.* **9**, ra100 [CrossRef Medline](#)
  14. Prsyazhna, O., Rudyk, O., and Eaton, P. (2012) Single atom substitution in mouse protein kinase G eliminates oxidant sensing to cause hypertension. *Nat. Med.* **18**, 286–290 [CrossRef Medline](#)
  15. Rudyk, O., Prsyazhna, O., Burgoyne, J. R., and Eaton, P. (2012) Nitroglycerin fails to lower blood pressure in redox-dead Cys42Ser PKGI $\alpha$  knock-in mouse. *Circulation* **126**, 287–295 [CrossRef Medline](#)
  16. Chan, S. L., and Baumbach, G. L. (2013) Deficiency of Nox2 prevents angiotensin II-induced inward remodeling in cerebral arterioles. *Front. Physiol.* **4**, 133 [Medline](#)
  17. Chan, S. L., and Baumbach, G. L. (2013) Nox2 deficiency prevents hypertension-induced vascular dysfunction and hypertrophy in cerebral arterioles. *Int. J. Hypertens.* **2013**, 793630 [Medline](#)
  18. Gray, S. P., Di Marco, E., Kennedy, K., Chew, P., Okabe, J., El-Osta, A., Calkin, A. C., Biessen, E. A., Touyz, R. M., Cooper, M. E., Schmidt, H. H., and Jandeleit-Dahm, K. A. (2016) Reactive oxygen species can provide atheroprotection via Nox4-dependent inhibition of inflammation and vascular remodeling. *Arterioscler. Thromb. Vasc. Biol.* **36**, 295–307 [CrossRef Medline](#)
  19. Kim, Y. M., Kim, S. J., Tatsunami, R., Yamamura, H., Fukai, T., and Ushio-Fukai, M. (2017) ROS-induced ROS release orchestrated by Nox4, Nox2, and mitochondria in VEGF signaling and angiogenesis. *Am. J. Physiol. Cell Physiol.* **312**, C749–C764 [CrossRef Medline](#)
  20. Patel, D., Lakhkar, A., and Wolin, M. S. (2017) Redox mechanisms influencing cGMP signaling in pulmonary vascular physiology and pathophysiology. *Adv. Exp. Med. Biol.* **967**, 227–240 [CrossRef Medline](#)
  21. Rashdan, N. A., and Lloyd, P. G. (2015) Fluid shear stress upregulates placental growth factor in the vessel wall via NADPH oxidase 4. *Am. J. Physiol. Heart Circ. Physiol.* **309**, H1655–H1666 [CrossRef Medline](#)
  22. Schiffrin, E. L. (2012) Vascular remodeling in hypertension: mechanisms and treatment. *Hypertension* **59**, 367–374 [CrossRef Medline](#)
  23. Blanton, R. M., Takimoto, E., Aronovitz, M., Thoonen, R., Kass, D. A., Karas, R. H., and Mendelsohn, M. E. (2013) Mutation of the protein kinase I  $\alpha$  leucine zipper domain produces hypertension and progressive left ventricular hypertrophy: a novel mouse model of age-dependent hypertensive heart disease. *J. Gerontol. A Biol. Sci. Med. Sci.* **68**, 1351–1355 [CrossRef Medline](#)
  24. Casteel, D. E., Boss, G. R., and Pilz, R. B. (2005) Identification of the interface between cGMP-dependent protein kinase  $\beta$  and its interaction partners TFII-I and IRAG reveals a common interaction motif. *J. Biol. Chem.* **280**, 38211–38218 [CrossRef Medline](#)
  25. Feil, R., Kellermann, J., and Hofmann, F. (1995) Functional cGMP-dependent protein kinase is phosphorylated in its catalytic domain at threonine-516. *Biochemistry* **34**, 13152–13158 [CrossRef Medline](#)
  26. Surks, H. K., Mochizuki, N., Kasai, Y., Georgescu, S. P., Tang, K. M., Ito, M., Lincoln, T. M., and Mendelsohn, M. E. (1999) Regulation of myosin phosphatase by a specific interaction with cGMP-dependent protein kinase  $\alpha$ . *Science* **286**, 1583–1587 [CrossRef Medline](#)
  27. Osborne, B. W., Wu, J., McFarland, C. J., Nickl, C. K., Sankaran, B., Casteel, D. E., Woods, V. L., Jr., Kornev, A. P., Taylor, S. S., and Dostmann, W. R. (2011) Crystal structure of cGMP-dependent protein kinase reveals novel site of interchain communication. *Structure* **19**, 1317–1327 [CrossRef Medline](#)
  28. Qin, L., Reger, A. S., Guo, E., Yang, M. P., Zwart, P., Casteel, D. E., and Kim, C. (2015) Structures of cGMP-dependent protein kinase (PKG)  $\alpha$  leucine zippers reveal an interchain disulfide bond important for dimer stability. *Biochemistry* **54**, 4419–4422 [CrossRef Medline](#)
  29. Moon, T. M., Tykocki, N. R., Sheehe, J. L., Osborne, B. W., Tegge, W., Brayden, J. E., and Dostmann, W. R. (2015) Synthetic peptides as cGMP-independent activators of cGMP-dependent protein kinase  $\alpha$ . *Chem. Biol.* **22**, 1653–1661 [CrossRef Medline](#)
  30. Moon, T. M., Sheehe, J. L., Nukareddy, P., Nausch, L. W., Wohlfahrt, J., Matthews, D. E., Blumenthal, D. K., and Dostmann, W. R. (2018) An N-terminally truncated form of cyclic GMP-dependent protein kinase  $\alpha$  (PKG I $\alpha$ ) is monomeric, autoinhibited, and provides a model for activation. *J. Biol. Chem.* **293**, 7916–7929 [CrossRef Medline](#)
  31. Han, J., Yen, S., Han, G., and Han, P. (1996) Quantitation of hydrogen peroxide using tris(2-carboxyethyl)phosphine. *Anal. Biochem.* **234**, 107–109 [CrossRef Medline](#)
  32. Tan, Z., Ihnat, P. M., Nayak, V. S., and Russell, R. J. (2012) Quantitative analysis of tris(2-carboxyethyl)phosphine by anion-exchange chromatography and evaporative light-scattering detection. *J. Pharm. Biomed. Anal.* **59**, 167–172 [CrossRef Medline](#)
  33. Alioua, A., Huggins, J. P., and Rousseau, E. (1995) PKG-I  $\alpha$  phosphorylates the  $\alpha$ -subunit and upregulates reconstituted GKCa channels from tracheal smooth muscle. *Am. J. Physiol.* **268**, L1057–L1063 [Medline](#)
  34. Kyle, B. D., Hurst, S., Swayze, R. D., Sheng, J., and Braun, A. P. (2013) Specific phosphorylation sites underlie the stimulation of a large conductance, Ca<sup>2+</sup>-activated K<sup>+</sup> channel by cGMP-dependent protein kinase. *FASEB J.* **27**, 2027–2038 [CrossRef Medline](#)
  35. Dostmann, W. R., Taylor, M. S., Nickl, C. K., Brayden, J. E., Frank, R., and Tegge, W. J. (2000) Highly specific, membrane-permeant peptide blockers of cGMP-dependent protein kinase I $\alpha$  inhibit no-induced cerebral dilation. *Proc. Natl. Acad. Sci. U.S.A.* **97**, 14772–14777 [CrossRef Medline](#)
  36. Francis, S. H., Smith, J. A., Colbran, J. L., Grimes, K., Walsh, K. A., Kumar, S., and Corbin, J. D. (1996) Arginine 75 in the pseudosubstrate sequence of type I $\beta$  cGMP-dependent protein kinase is critical for autoinhibition, although autophosphorylated serine 63 is outside this sequence. *J. Biol. Chem.* **271**, 20748–20755 [CrossRef Medline](#)
  37. Heil, W. G., Landgraf, W., and Hofmann, F. (1987) A catalytically active fragment of cGMP-dependent protein kinase: occupation of its cGMP-binding sites does not affect its phosphotransferase activity. *Eur. J. Biochem.* **168**, 117–121 [CrossRef Medline](#)
  38. Ruth, P., Landgraf, W., Keilbach, A., May, B., Egleme, C., and Hofmann, F. (1991) The activation of expressed cGMP-dependent protein kinase isozymes I $\alpha$  and I $\beta$  is determined by the different amino-termini. *Eur. J. Biochem.* **202**, 1339–1344 [CrossRef Medline](#)
  39. Aitken, A., Hemmings, B. A., and Hofmann, F. (1984) Identification of the residues on cyclic GMP-dependent protein kinase that are autophosphorylated in the presence of cyclic amp and cyclic GMP. *Biochim. Biophys. Acta* **790**, 219–225 [CrossRef Medline](#)
  40. Alverdi, V., Mazon, H., Versluis, C., Hemrika, W., Esposito, G., van den Heuvel, R., Scholten, A., and Heck, A. J. (2008) cGMP-binding prepares PKG for substrate binding by disclosing the C-terminal domain. *J. Mol. Biol.* **375**, 1380–1393 [CrossRef Medline](#)
  41. Lee, E., Hayes, D. B., Langsetmo, K., Sundberg, E. J., and Tao, T. C. (2007) Interactions between the leucine-zipper motif of cGMP-dependent protein kinase and the C-terminal region of the targeting subunit of myosin light chain phosphatase. *J. Mol. Biol.* **373**, 1198–1212 [CrossRef Medline](#)
  42. Zhou, G. P. (2011) The structural determinations of the leucine zipper coiled-coil domains of the cGMP-dependent protein kinase I $\alpha$  and its interaction with the myosin binding subunit of the myosin light chains phosphatase. *Protein Pept. Lett.* **18**, 966–978 [CrossRef Medline](#)
  43. Kalyanaraman, H., Zhuang, S., Pilz, R. B., and Casteel, D. E. (2017) The activity of cGMP-dependent protein kinase I $\alpha$  is not directly regulated by oxidation-induced disulfide formation at cysteine 43. *J. Biol. Chem.* **292**, 8262–8268 [CrossRef Medline](#)
  44. Nausch, L. W., Ledoux, J., Bonev, A. D., Nelson, M. T., and Dostmann, W. R. (2008) Differential patterning of cGMP in vascular smooth muscle cells revealed by single GFP-linked biosensors. *Proc. Natl. Acad. Sci. U.S.A.* **105**, 365–370 [CrossRef Medline](#)
  45. Schlossmann, J., and Desch, M. (2009) cGK substrates. *Handb. Exp. Pharmacol.* **163**–193 [CrossRef](#)
  46. Ruth, P., Pfeifer, A., Kamm, S., Klatt, P., Dostmann, W. R., and Hofmann, F. (1997) Identification of the amino acid sequences responsible for high affinity activation of cGMP kinase I $\alpha$ . *J. Biol. Chem.* **272**, 10522–10528 [CrossRef Medline](#)
  47. Kim, J. J., Lorenz, R., Arold, S. T., Reger, A. S., Sankaran, B., Casteel, D. E., Herberg, F. W., and Kim, C. (2016) Crystal structure of PKG I:cGMP

## Oxidation-dependent activation of PKG Ia Cys-117

- complex reveals a cGMP-mediated dimeric interface that facilitates cGMP-induced activation. *Structure* **24**, 710–720 [CrossRef](#) [Medline](#)
48. Nakamura, T., Ranek, M. J., Lee, D. I., Shalkey Hahn, V., Kim, C., Eaton, P., and Kass, D. A. (2015) Prevention of PKG1 $\alpha$  oxidation augments cardioprotection in the stressed heart. *J. Clin. Invest.* **125**, 2468–2472 [CrossRef](#) [Medline](#)
49. Warren, E. A., Netterfield, T. S., Sarkar, S., Kemp, M. L., and Payne, C. K. (2015) Spatially-resolved intracellular sensing of hydrogen peroxide in living cells *Sci. Rep.* **5**, 16929 [CrossRef](#) [Medline](#)
50. Brewer, T. F., Garcia, F. J., Onak, C. S., Carroll, K. S., and Chang, C. J. (2015) Chemical approaches to discovery and study of sources and targets of hydrogen peroxide redox signaling through NADPH oxidase proteins. *Annu. Rev. Biochem.* **84**, 765–790 [CrossRef](#) [Medline](#)
51. Karplus, P. A. (2015) A primer on peroxiredoxin biochemistry. *Free Radic. Biol. Med.* **80**, 183–190 [CrossRef](#) [Medline](#)
52. Waterhouse, A. M., Procter, J. B., Martin, D. M., Clamp, M., and Barton, G. J. (2009) Jalview version 2—a multiple sequence alignment editor and analysis workbench. *Bioinformatics* **25**, 1189–1191 [CrossRef](#) [Medline](#)
53. Sievers, F., Wilm, A., Dineen, D., Gibson, T. J., Karplus, K., Li, W., Lopez, R., McWilliam, H., Remmert, M., Söding, J., Thompson, J. D., and Higgins, D. G. (2011) Fast, scalable generation of high-quality protein multiple sequence alignments using Clustal omega. *Mol. Syst. Biol.* **7**, 539 [Medline](#)